Online Supplementary Material to: Analysis of a generic model of eukaryotic cell cycle regulation

Attila Csikász-Nagy*,#, Dorjsuren Battogtokh*, Katherine C. Chen*, Béla Novák# & John J. Tyson*

*Department of Biological Sciences, Virginia Polytechnic Institute and State University, Blacksburg, Virginia 24061-0406, USA

#Molecular Network Dynamics Research Group of the Hungarian Academy of Sciences and Department of Agricultural and Chemical Technology, Budapest University of Technology and Economics, Gellert ter 4, H-1521 Budapest, Hungary;

01/04/06

Corresponding author: John J. Tyson, tyson@vt.edu,

Tel: 540-231-4662, Fax: 540-231-9307

A. The model: differential equations and parameter sets

In Table SI we present the differential and algebraic equations that define our generic model of the cell cycle. In Table SII we list the particular parameter values that we propose for the organisms modeled in this paper. The 'G2 module' refers to the parameter values used to model Wee1 and Cdc25 activity in the extended budding-yeast and mammalian-cell models.

In the models for specific organisms, some modules are missing, in which case their associate rate constants are set to 0 (except for those that would give a division by zero; these rate constants we set to an artificial number). The '.set files' on our web site provide convenient electronic versions of these parameter, with the artificial numbers included. To create the bifurcation diagram for APC-A mutants we deleted the equation of *APCP* and used *APCP* = 0.1 (10% of total activity) as a parameter.

B. Frog egg

From the equations in Table SI and the 'Xenopus embryo' parameter set in Table SII, we computed a one-parameter bifurcation diagram (Fig. S1), which is qualitatively similar to the corresponding diagram in Borisuk & Tyson (1). 'Rate constant for cyclin synthesis' in their diagram is equivalent to k_{sbp}**mass* in our model.

C. Fission yeast mutants

Fig. S2A: Wild-type fission yeast cell. For comparison.

Fig. S2B: *cig2D*. Cig2 = CycA (modules 11-12-13). The *cig2*-deletion mutant is viable and roughly the same size as wild-type cells (2). Comparing this mutant to wild-type cells (panel A), the G1 steady state persists to larger cell mass, i.e., cells must grow to a larger size before they leave G1 phase. The critical size for leaving G2 (the SNIPER bifurcation point) remains the same, so the mutant cells are about the same size as wild type.

Fig. S2C: *cig2D rum1D*. Rum1 = CKI (modules 6, 8, 9, 12). This double-deletion mutant is also viable and similar to wild type (3). The G1 steady state moves back to smaller cell size. Although the double-deletion mutant is predicted to be similar in size to wild-type cells, the amplitude of the limit cycle is reduced. As a consequence, actCycB does not drop as low as in wild-type cells and G1 phase is even shorter.

Fig. S2D: *wee1$^-$ cdc25D*. When both the G2 inhibitor and activator are missing, cells are viable but exhibit an unusual, trimodal distribution of cycle times (4,5). In the bifurcation diagram, the SNIPER is missing and mitotic oscillations are initiated from a supercritical Hopf bifurcation on the M-branch of steady states. Consequently, after passing the G2 checkpoint, the control system is attracted to a stable mitotic state. At a slightly larger size, the stable mitotic state gives way to oscillations whose amplitudes are too small (at first) to carry the cell successfully out of M phase. Finally, when the cell grows large enough, a large amplitude oscillation in actCycB induces cell division. The distribution of cycle times in a population of cells is quantized (bimodal in this deterministic model) because the number of small amplitude oscillations experienced by a cell depends on its birth size.

Fig. S2E: *wee1*$^{-}$ *rum1D*. In the single deletion mutant, *rum1D* (6), the G1 steady state is moved to small size (not shown), but the mutant cells cycle just like wild type. In the double mutant, *wee1*^{ts} *rum1D*, both G1 and G2 steady states are moved to very small size. As a result, when *wee1*^{ts} *rum1D* cells are transferred from 25^{o}C (Wee1 active, cells viable and wild-type size) to 35^{o}C (Wee1 inactive), the cells become smaller and smaller each division cycle and eventually die because they are too small to hold a dividing nucleus (6). In simulations, the mutant stabilizes at one-fourth wild-type size, which is probably too small to be viable.

Fig. S2F: *cdc13*$^{+/-}$. Assuming that heterozygous diploid cells for the *cdc13*$^{-}$ allele will have ½ the wild-type amount of Cdc13 protein, we find in the one-parameter bifurcation diagram a region of endoreplication cycles at small cell mass (~1 au, about half the size of wild-type cells), as well as mitotic cycles at about twice the size of wild type cells. To our knowledge, no one has ever looked for signs of endoreplication in these cells at very small size (e.g., after spore germination).

C. Budding yeast mutants

C.1. Mutants of G1 phase regulation

Fig. S3A and B: variable expression of *CDH1* and *SIC1*. As levels of expression of *CDH1* and *SIC1* decrease, oscillations move to smaller cell mass, and oscillation periods get longer. Balanced growth and division is achieved in the 'oscillator' domain, see Figs. 5C and D in the main text. On Fig. S3A, as Cdh1 activity decreases, the oscillations move from a SNIPER bifurcation (red line) to large amplitude oscillations derived from a CF

(cyclic fold) bifurcation (blue line). (This 'move' is accomplished by a complicated sequence of bifurcations not indicated in the diagram at this scale.) For decreasing levels of Sic1 (Fig. S2B), the wild-type SNIPER bifurcation (upper red line) switches over to a SNIPER on a different SN branch (lower red line), again by a complicated sequence of bifurcations not indicated on the diagram.

C.2. Mutants of mitotic exit regulation

Fig. S3C and D: variable expression of *CDC20* and *CDC14*. As levels of expression of *CDC20* and *CDC14* decrease, oscillations disappear at a CF bifurcation (blue line). These bifurcation diagrams are quite similar, confirming that the mutations cause quite similar phenotypes (mitotic arrest). The major difference between the mutants, namely the different levels of CycB in the arrested state (Fig. 5E and F), cannot be visualized on these two-parameter diagrams.

C.3. Morphogenetic checkpoint mutants

Fig. S4A: *cdc24^{ts}*. The morphogenetic checkpoint (7) is turned on in *cdc24^{ts}* cells at the restrictive temperature, because they cannot form buds (8). Activation of the checkpoint causes activation of Swe1, which introduces a G2 delay by phosphorylating Cdk1. Following Ciliberto et al. (9) we introduced Swe1 and Mih1 (aka: Wee1 and Cdc25) into our model, using Ciliberto's parameter values for the *cdc24^{ts}* mutation. Our bifurcation diagram (Fig. S4A) shows that a stable G2 steady state appears, but it is mostly hidden by the stable G1 steady state; just a small stable branch of the G2 attractor is visible for

growing cells. Nonetheless, the G2 module extends the periods of oscillations, and as we see on the simulation curve, the cells enter mitosis with a long delay. Cells grow very large because the MDT cannot be balanced by the cell-cycle oscillation period.

Fig. S4B: *hsl1D mih1D*. Cells that are deleted for both Hsl1, the inhibitor of Swe1, and Mih1, the phosphatase that opposes Swe1, have a very stable G2 attractor (Fig. S4B) extending to very large cell mass. These cells are inviable (10).

D. Mammalian cell cycle results

Fig. S5A: Wild-type cells without the G2 module. For comparison with (11).

Fig. S5B: Wild-type cells with the G2 module. A more realistic model than (11), because mammalian cells have a functional G2 checkpoint mechanism.

Fig. S5C: *cycED*. Cells are viable and only slightly larger than wild type. By comparison, *cycDD* cells in our model (Fig. 8C in main text) are considerably larger than wild type.

Supplementary figure legends

Fig. S1. One-parameter bifurcation diagram for the 'Xenopus embryo' parameter set.

Fig. S2. One-parameter bifurcation diagrams of fission yeast mutants. (**A)** WT **(**Wild Type) parameter values. (Same as Fig. 2A of main text.) (**B)** $k_{sapp} = 0$, (**C)** $k_{sapp} = k_{sip} = 0$, (**D)** $k_{weepp} = 0.05\ min^{-1}$, $k_{25pp} = 0.001\ min^{-1}$ (10% of WT values), (**E**) $k_{weepp} = 0.05\ min^{-1}$, $k_{sip} = 0$, (**F**) $k_{sbp} = 0.01\ min^{-1}$ (50% of WT value).

Fig. S3. Two-parameter bifurcation diagrams of budding yeast mutants. Varying levels of G1 antagonists (**A**: k_{ah1p} and k_{ah1pp}; **B**: k_{sip} and k_{sipp} changed together), and mitotic-exit regulators (**C**: k_{s20p} and k_{s20pp}; **D**: k_{ah1pp}, k_{afi} and k_{14di} changed together). Ordinates are normalized to have wild-type cells at level 10^0 on each plot. Black lines (solid or dashed) denote pairs of SN loci that meet at a CUSP point; red line = SNIPER locus; blue line = CF locus; purple line = Hopf bifurcation locus. In the oscillatory domains, period (T) is indicated by the color scale.

Fig. S4. Morphogenesis checkpoint mutants of budding yeast. One-parameter bifurcation diagrams of the generic model with budding-yeast parameter values + the morphogenetic checkpoint module (#5). (**A**) *cdc24*^{ts}. Simulation curve (MDT = 120 min) is initiated from wild-type cell mass at birth. The *cdc24*^{ts} mutant is unable to make a bud; consequently, Wee1 activity is activated and Cdc25 activity is inhibited. Cells are delayed

in G2 phase for about 2 h, but they eventually divide at a large size, giving rise to one binucleate cell and one anucleate cell (10). (**B**) *hsl1D mih1D*. Same as A, except $k_{25p} = k_{25pp} = 0$. This mutant is inviable (12). In our model, it is stuck in G2 phase and grows very large (and presumably dies). On the far right, for comparison purposes, are the corresponding diagrams in Ciliberto et al. (9).

Fig. S5. One-parameter bifurcation diagrams and simulations of mammalian cell cycles. Wild-type cells without G2 module **(A),** and with G2 module **(B)**. Red curves: simulations for MDT = 14 h. (**C**) *cycED* mutant: $k_{sep} = k_{sepp} = 0$.

Table SI. Equations

Cdk/cyclin complexes:

$$\frac{dactCycA}{dt} = \left(k_{sap} + k_{sapp} \cdot TF_E\right) \cdot mass + \left(V_{di} + k_{dia}\right) \cdot Tri_A - \left(V_{da} + k_{asa} \cdot freeCKI\right) \cdot actCycA$$

$$\frac{dactCycB}{dt} = V_{sb} \cdot mass + V_{25} \cdot \left(CycB - Tri_B - actCycB\right) + \left(k_{dib} + V_{di}\right) \cdot \left(CycB - preMPF - actCycB\right) - \left(V_{db} + V_{wee} + k_{asb} \cdot freeCKI\right) \cdot actCycB$$

$$\frac{dactCycE}{dt} = \left(k_{sep} + k_{sepp} \cdot TF_E\right) \cdot mass + \left(V_{di} + k_{die}\right) \cdot Tri_E - \left(V_{de} + k_{ase} \cdot freeCKI\right) \cdot actCycE$$

$$\frac{dCycA}{dt} = \left(k_{sap} + k_{sapp} \cdot TF_E\right) \cdot mass - V_{da} \cdot CycA$$

$$\frac{dCycB}{dt} = V_{sb} \cdot mass - V_{db} \cdot CycB$$

$$\frac{dCycE}{dt} = \left(k_{sep} + k_{sepp} \cdot TF_E\right) \cdot mass - V_{de} \cdot CycE$$

Cdk regulators:

$$\frac{dCdh1}{dt} = \frac{\left(k_{ah1p} + k_{ah1pp} Cdc14\right) \cdot \left(1 - Cdh1\right)}{J_{ah1} + 1 - Cdh1} - \frac{\left(k_{ih1p} + k_{ih1pp} actCycA + k_{ih1ppp} actCycB + k_{ih1pppp} actCycE + k_{ih1ppppp} CycD\right) \cdot Cdh1}{J_{ih1} + Cdh1}$$

$$\frac{dCKI}{dt} = V_{si} - V_{di} \cdot CKI$$

$$\frac{dTri_B}{dt} = k_{asb} \cdot \left(CycB - Tri_B\right) \cdot freeCKI - \left(k_{dib} + V_{db} + V_{di}\right) \cdot Tri_B$$

$$\frac{dpreMPF}{dt} = V_{wee} \cdot \left(CycB - preMPF\right) - \left(V_{25} + V_{db}\right) \cdot preMPF$$

$$\frac{dAPCP}{dt} = \frac{k_{aAPC} \cdot actCycB \cdot \left(1 - APCP\right)}{J_{aAPC} + 1 - APCP} - \frac{k_{iAPC} \cdot APCP}{J_{iAPC} + APCP}$$

$$\frac{dCdc20_A}{dt} = \frac{k_{a20} \cdot APCP \cdot \left(Cdc20_T - Cdc20_A\right)}{J_{a20} + Cdc20_T - Cdc20_A} - \left(\frac{k_{i20}}{J_{i20} + Cdc20_A} + k_{d20}\right) \cdot Cdc20_A$$

$$\frac{dCdc20_T}{dt} = \frac{k_{s20p} + k_{s20pp} \cdot actCycB^n}{J_{20}^n + actCycB^n} - k_{d20} \cdot Cdc20_T$$

where:

$$CycD = CycD^{0} \cdot mass$$

$$V_{atf} = k_{atfp} + k_{atfpp} \cdot actCycA + k_{atfppp} \cdot actCycE + k_{atfpppp} \cdot CycD$$

$$TF_{E} = G\left(V_{atf}, k_{itfp} + k_{itfpp} \cdot actCycB + k_{itfppp} \cdot actCycA, J_{atf}, J_{itf}\right)$$

$$V_{de} = k_{dep} + k_{depp} \cdot actCycE + k_{deppp} \cdot actCycA + k_{depppp} \cdot actCycB$$

$$V_{da} = k_{dap} + k_{dapp} \cdot Cdc20_{A} + k_{dappp} \cdot Cdc20_{T}$$

$$Cdc14 = Cdc20_{A}$$

$$TF_{I} = G\left(k_{afi} \cdot Cdc14, k_{ifip} + k_{ifipp} \cdot actCycB, J_{afi}, J_{ifi}\right)$$

$$V_{si} = k_{sip} + k_{sipp} \cdot TF_{I}$$

$$V_{di} = \frac{k_{dip} + k_{dipp} \cdot actCycA + k_{dippp} \cdot actCycB + k_{dipppp} \cdot actCycE + k_{dippppp} \cdot CycD}{1 + \left(Cdc14/J_{14di}\right)}$$

$$[\text{Cdk1:CycB:CKI}] = CycB - actCycB - preMPF$$

$$[\text{Cdk1P:CycB}] = CycB - actCycB - Tri_{B}$$

$$Tri_{A} = CycA - actCycA$$

$$Tri_{E} = CycE - actCycE$$

$$freeCKI = CKI - Tri_{B} - Tri_{A} - Tri_{E}$$

$$TF_{B} = G\left(k_{afb} \cdot actCycB, k_{ifb}, J_{afb}, J_{ifb}\right)$$

$$V_{sb} = k_{sbp} + k_{sbpp} \cdot TF_{B}$$

$$V_{db} = k_{dbp} + k_{dbpp} \cdot Cdh1 + k_{dbppp} \cdot Cdc20_{A}$$

$$Wee1 = G\left(k_{aweep} + k_{aweepp} \cdot Cdc14, k_{iwee} \cdot actCycB, J_{awee}, J_{iwee}\right)$$

$$V_{wee} = k_{weep} + k_{weepp} \cdot Wee1$$

$$Cdc25 = G\left(k_{a25} \cdot actCycB, k_{i25p} + k_{i25pp} \cdot Cdc14, J_{a25}, J_{i25}\right)$$

$$V_{25} = k_{25p} + k_{25pp} \cdot Cdc25$$

G(…) is the Goldbeter-Koshland function:

$$B\left(A_1, A_2, A_3, A_4\right) = A_2 - A_1 + A_3 \cdot A_2 + A_4 \cdot A_1$$

$$G\left(A_1, A_2, A_3, A_4\right) = \frac{2 \cdot A_4 \cdot A_1}{B\left(A_1, A_2, A_3, A_4\right) + \sqrt{B\left(A_1, A_2, A_3, A_4\right)^{2} - 4 \cdot \left(A_2 - A_1\right) \cdot A_4 \cdot A_1}}$$

For simulations of periodic cell cycles:

Growth: $\frac{dmass}{dt} = \mu \cdot mass$, where μ = ln2/MDT, MDT=mass-doubling time

Division: $mass \rightarrow mass/2$, when *actCycB* decreases to 0.1 (fission yeast), 0.2 (budding yeast), 0.3 (mammalian cell)

Table SII. Parameter sets (dimension of k's is min^{-1})

parameter	budding yeast	mammalian cells	fission yeast	G2 module	Xenopus embryos
J_{20}	100	100	0.05	-	-
J_{a20}	10	0.005	0.001	-	0.1
J_{a25}	-	-	0.01	0.1	0.1
J_{aAPC}	0.1	0.01	0.001	-	0.01
J_{afb}	0.1	0.1	-	-	-
J_{afi}	10	-	-	-	-
J_{ah1}	0.03	0.01	0.01	-	-
J_{atf}	0.01	0.01	0.01	-	-
J_{awee}	-	-	0.01	0.05	0.3
J_{i20}	10	0.005	0.001	-	0.1
J_{i25}	-	-	0.01	0.1	0.1
J_{iAPC}	0.1	0.01	0.001	-	0.01
J_{ifb}	0.1	0.1	-	-	-
J_{ifi}	10	-	-	-	-
J_{ih1}	0.03	0.01	0.01	-	-
J_{itf}	0.01	0.01	0.01	-	-
J_{iwee}	-	-	0.01	0.05	0.3
J_{14di}	0.0833	-	-	-	-
k_{25p}	-	-	0.001	0.05	0.1
k_{25pp}	-	-	1	0.5	1.9
k_{a20}	1	0.0833	0.2	-	0.1
k_{a25}	-	-	1	1	1
k_{aAPC}	0.1	0.0117	0.2	-	2
k_{afb}	1	0.167	-	-	-
k_{afi}	6	-	-	-	-
k_{ah1p}	0.01	0.175	5	-	-
k_{ah1pp}	0.8	2.33	50	-	-
k_{asa}	50	16.7	500	-	-
k_{asb}	65	-	1000	-	-
k_{ase}	-	16.7	-	-	-
k_{atfp}	-	-	1.5	-	-
k_{atfpp}	0.76	0.05	-	-	-
k_{atfppp}	0.76	0.0833	-	-	-
$k_{atfpppp}$	3.8	0.055	-	-	-
k_{aweep}	-	-	0.25	0.3	0.1
k_{aweepp}	-	-	0.25	-	-
k_{d20}	0.05	0.025	0.1	-	1
k_{dap}	0.01	0.000333	0.01	-	-
k_{dapp}	0.16	0.333	2	-	-
k_{dappp}	-	-	0.02	-	-
k_{dbp}	0.003	0.000833	0.02	-	0.015
k_{dbpp}	0.4	0.333	0.75	-	-

parameter	budding yeast	mammalian cells	fission yeast	G2 module	Xenopus embryos
k_{dbppp}	0.15	0.0167	1.5	-	0.985
k_{dep}	0.12	0.00167	-	-	-
k_{depp}	-	0.0167	-	-	-
k_{deppp}	-	0.167	-	-	-
k_{depppp}	-	0.167	-	-	-
k_{dia}	0.06	0.167	1	-	-
k_{dib}	0.05	-	1	-	-
k_{die}	-	0.167	-	-	-
k_{dip}	0.02	0.167	0.1	-	-
k_{dipp}	0.2	0.833	2	-	-
k_{dippp}	0.9	1.67	100	-	-
k_{dipppp}	0.12	0.833	-	-	-
$k_{dippppp}$	0.66	-	1	-	-
k_{i20}	0.05	0.0417	0.05	-	0.095
k_{i25p}	-	-	0.25	0.3	0.125
k_{i25pp}	-	-	0.25	-	-
k_{iAPC}	0.15	0.03	0.08	-	0.15
k_{ifb}	0.15	0.0167	-	-	-
k_{ifip}	0.008	-	-	-	-
k_{ifipp}	0.05	-	-	-	-
k_{ih1p}	0.001	-	1	-	-
k_{ih1pp}	0.64	0.2	40	-	-
k_{ih1ppp}	0.1	0.667	40	-	-
$k_{ih1pppp}$	0.032	-	-	-	-
$k_{ih1ppppp}$	0.01	-	40	-	-
k_{itfp}	0.6	0.0417	1	-	-
k_{itfpp}	8	0.0167	-	-	-
k_{itfppp}	-	0.0167	10	-	-
k_{iwee}	-	-	1	1	3
k_{s20p}	0.001	-	0.005	-	1
k_{s20pp}	10	2.5	0.1	-	-
k_{sap}	0.0008	-	-	-	-
k_{sapp}	0.005	0.00417	0.02	-	-
k_{sbp}	0.004	0.00167	0.02	-	0.1
k_{sbpp}	0.04	0.005	-	-	-
k_{sep}	-	0.00133	-	-	-
k_{sepp}	0.15	0.05	-	-	-
k_{sip}	0.036	.333	0.3	-	-
k_{sipp}	0.24	-	-	-	-
k_{weep}	-	-	0.05	0.2	0.1
k_{weepp}	-	-	0.5	2	0.9
n	1	1	4	-	-
$CycD^0$	0.108	0.5	0.05	-	-

References

1. Borisuk, M. T. and J. J. Tyson. 1998. Bifurcation analysis of a model of mitotic control in frog eggs. J. Theor. Biol. 195:69-85.

2. Bueno, A. and P. Russell. 1993. Two fission yeast B-type cyclins, Cig2 and Cdc13, have different functions in mitosis. Mol. Cell. Biol. 13:2286-2297.

3. Martin-Castellanos, C., M. Blanco, J. M. de Prada, and S. Moreno. 2000. The Puc1 cyclin regulates the G1 phase of the fission yeast cell cycle in response to cell size. Mol. Biol. Cell 11:543-554.

4. Enoch, T., K. L. Gould, and P. Nurse. 1991. Mitotic checkpoint control in fission yeast. In The Cell Cycle. D.Beach, B.Stillman, and J.D.Watson, editors. Cold Spring Harbor Laboratory Press. Cold Spring Harbor. 409-416.

5. Sveiczer, A., B. Novak, and J. M. Mitchison. 1996. The size control of fission yeast revisited. J. Cell Sci. 109:2947-2957.

6. Moreno, S., K. Labib, J. Correa, and P. Nurse. 1994. Regulation of the cell cycle timing of Start in fission yeast by the *rum1*$^+$ gene. J. Cell Sci. Suppl. 18:63-68.

7. Lew, D. J. 2003. The morphogenesis checkpoint: how yeast cells watch their figures. Curr. Opin. Cell Biol. 15:648-653.

8. Sloat, B. F., A. Adams, and J. R. Pringle. 1981. Roles of the Cdc24 Gene-Product in Cellular Morphogenesis During the Saccharomyces-Cerevisiae Cell-Cycle. J. Cell Biol 89:395-405.

9. Ciliberto, A., B. Novak, and J. J. Tyson. 2003. Mathematical model of the morphogenesis checkpoint in budding yeast. J. Cell Biol 163:1243-1254.

10. McMillan, J. N., M. S. Longtine, R. A. Sia, C. L. Theesfeld, E. S. G. Bardes, J. R. Pringle, and D. J. Lew. 1999. The morphogenesis checkpoint in *Saccharomyces cerevisiae*: cell cycle control of Swe1p degradation by Hsl1p and Hsl7p. Mol. Cell. Biol. 19:6929-6939.

11. Novak, B. and J. J. Tyson. 2004. A model for restriction point control of the mammalian cell cycle. J. Theor. Biol. 230:563-579.

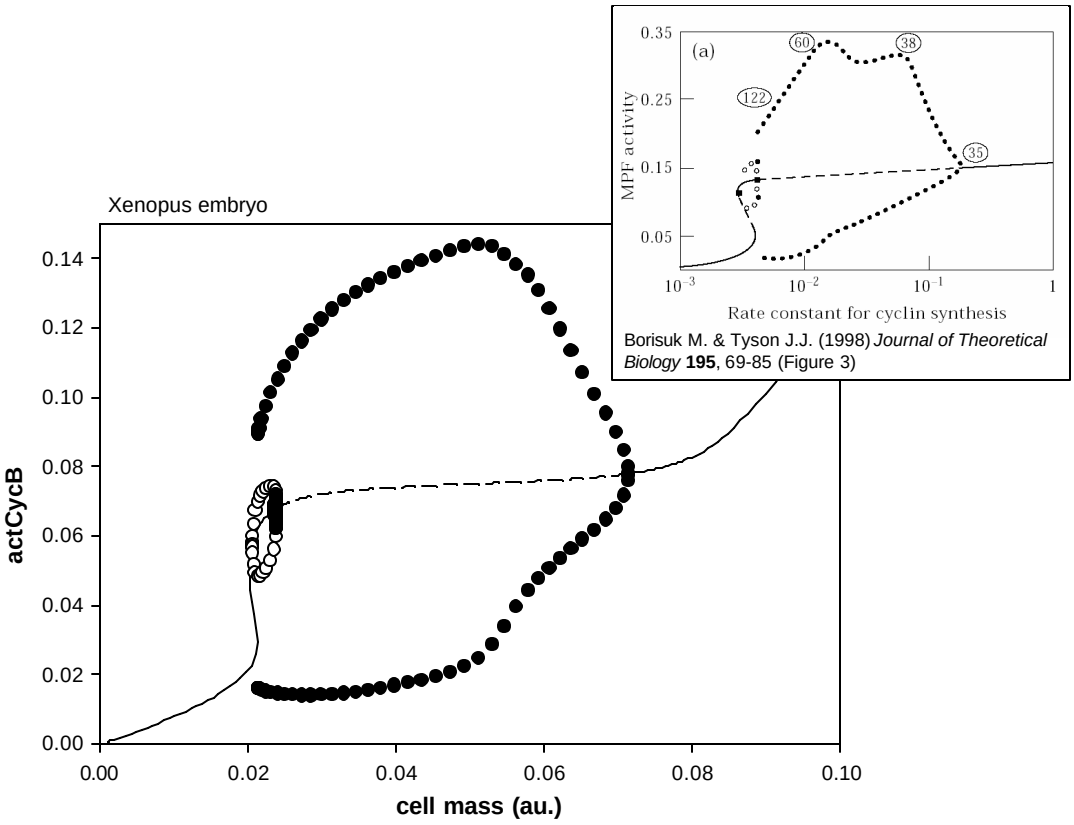

Figure S1. One-parameter bifurcation diagram for the 'Xenopus embryo' parameter set.

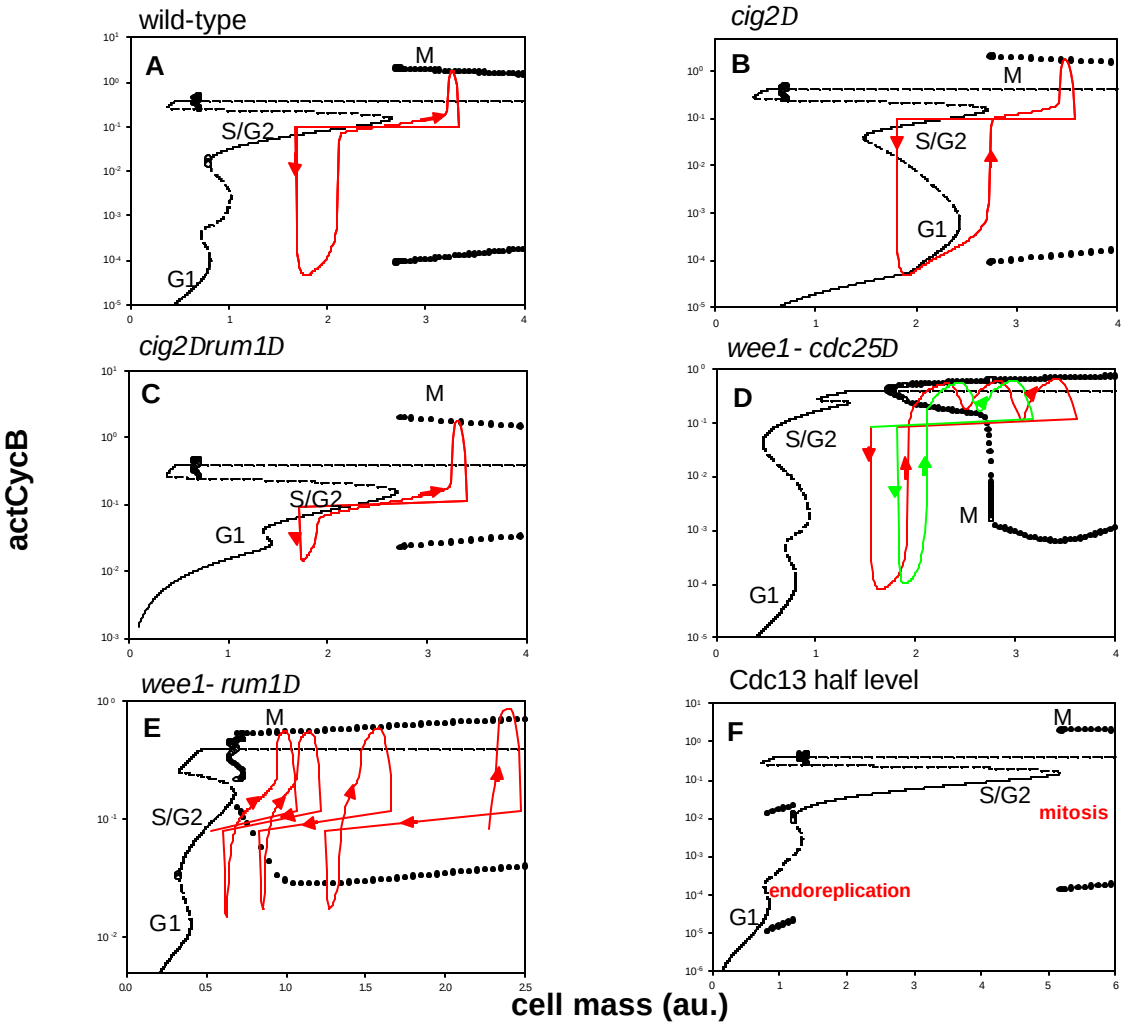

Figure S2. One-parameter bifurcation diagrams of fission yeast mutants. (**A)** WT **(**Wild Type) parameter values. (Same as Fig. 2A of main text.) (**B)** $k_{sapp} = 0$, (**C)** $k_{sapp} = k_{sip} = 0$, (**D)** $k_{weepp} = 0.05$ min^{-1}, $k_{25pp} = 0.001$ min^{-1} (10% of WT values), (**E**) $k_{weepp} = 0.05$ min^{-1}, $k_{sip} = 0$, (**F**) $k_{sbp} = 0.01$ min^{-1} (50% of WT value).

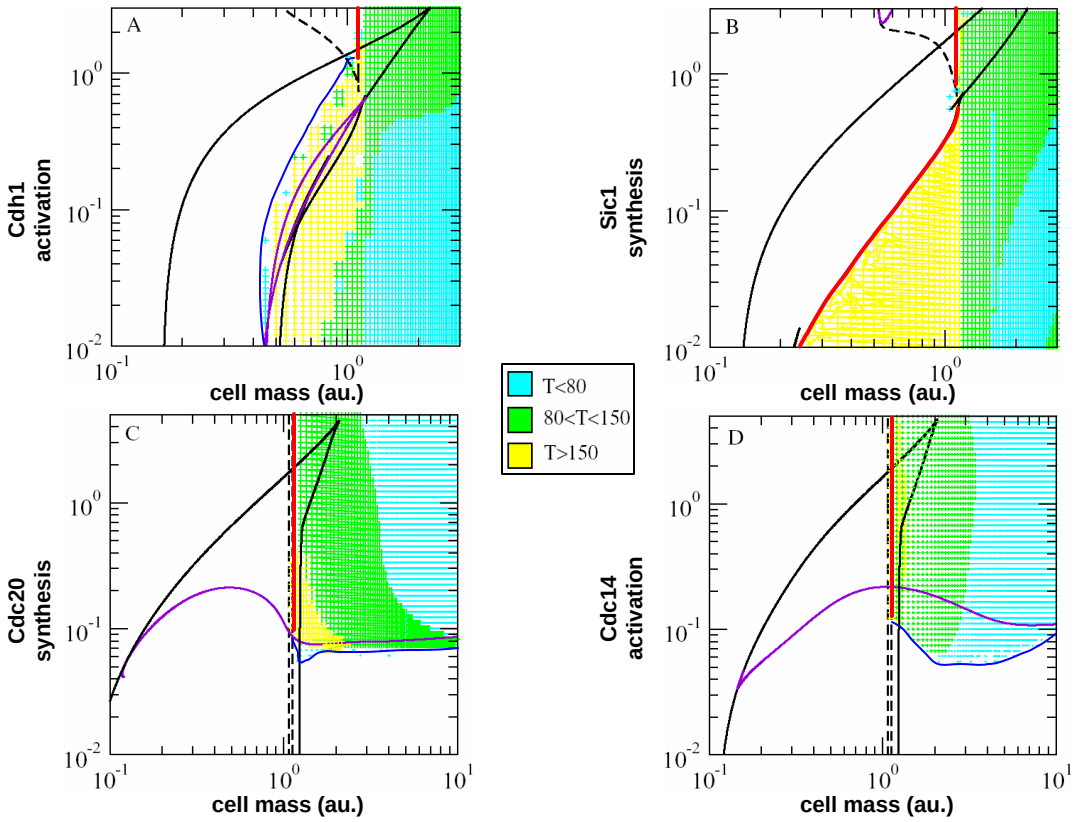

Figure S3. Two-parameter bifurcation diagrams of budding yeast mutants. Varying levels of G1 antagonists (**A**: k_{ah1p} and k_{ah1pp}; **B**: k_{sip} and k_{sipp} changed together), and mitotic-exit regulators (**C**: k_{s20p} and k_{s20pp}; **D**: k_{ah1pp}, k_{afi} and k_{14di} changed together). Ordinates are normalized to have wild-type cells at level 10^0 on each plot. Black lines (solid or dashed) denote pairs of SN loci that meet at a CUSP point; red line = SNIPER locus; blue line = CF locus; purple line = Hopf bifurcation locus. In the oscillatory domains, period (T) is indicated by the color scale.

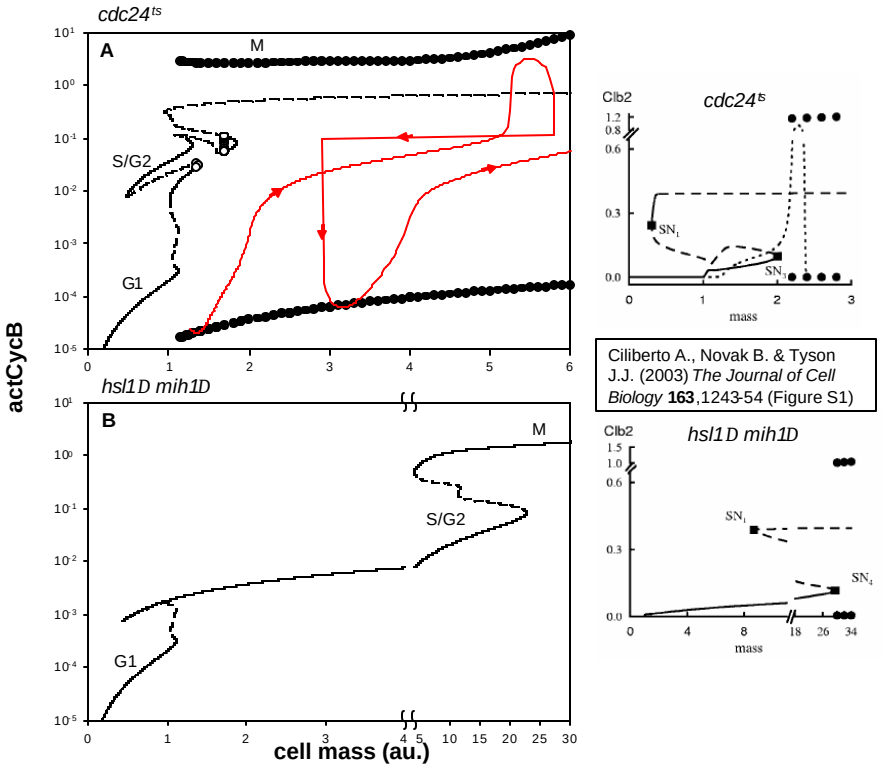

Figure S4. Morphogenesis checkpoint mutants of budding yeast. One-parameter bifurcation diagrams of the generic model with budding-yeast parameter values + the morphogenetic checkpoint module (#5). (**A**) *cdc24*^{ts}. Simulation curve (MDT = 120 min) is initiated from wild-type cell mass at birth. The *cdc24*^{ts} mutant is unable to make a bud; consequently, Wee1 activity is activated and Cdc25 activity is inhibited. Cells are delayed in G2 phase for about 2 h, but they eventually divide at a large size, giving rise to one binucleate cell and one anucleate cell (10). (**B**) *hsl1D mih1D*. Same as A, except $k_{25p} = k_{25pp} = 0$. This mutant is inviable (12). In our model, it is stuck in G2 phase and grows very large (and presumably dies). On the far right, for comparison purposes, are the corresponding diagrams in Ciliberto et al. (9).

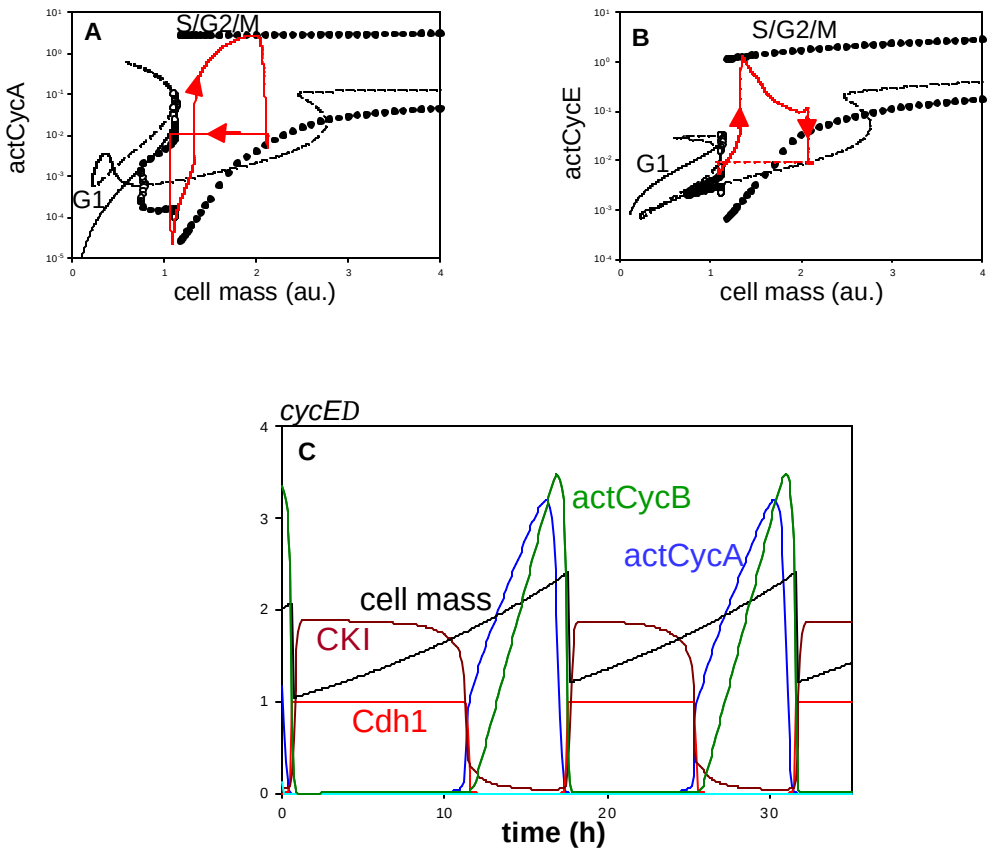

Figure S5. One-parameter bifurcation diagrams and simulations of mammalian cell cycles. Wild-type cells without G2 module **(A),** and with G2 module **(B)**. Red curves: simulations for MDT = 14 h. (**C**) *cycED* mutant: $k_{sep} = k_{sepp} = 0$.